

Research Article

Open Access



# Immobilized enzymatic alcohol oxidation as a versatile reaction module for multienzyme cascades

Kesheng Fu<sup>1</sup>, Lele Dong<sup>1</sup>, Pengbo Liu<sup>1</sup>, Liya Zhou<sup>1</sup>, Guanhua Liu<sup>1</sup>, Jing Gao<sup>1</sup>, Bingjun Gao<sup>1</sup>, Yunting Liu<sup>1,2,\*</sup>, Yanjun Jiang<sup>1,2,\*</sup>

<sup>1</sup>School of Chemical Engineering and Technology, Hebei University of Technology, Tianjin 300130, China.

<sup>2</sup>Tianjin Key Laboratory of Chemical Process Safety, Hebei University of Technology, Tianjin 300401, China.

\*Correspondence to: Prof. Yunting Liu, School of Chemical Engineering and Technology, Hebei University of Technology, 5340 Xiping Road, Tianjin 300130, China. E-mail: ytliu@hebut.edu.cn; Prof. Yanjun Jiang, School of Chemical Engineering and Technology, Hebei University of Technology, 5340 Xiping Road, Tianjin 300130, China. E-mail: yanjunjiang@hebut.edu.cn.

**How to cite this article:** Fu K, Dong L, Liu P, Zhou L, Liu G, Gao J, Gao B, Liu Y, Jiang Y. Immobilized enzymatic alcohol oxidation as a versatile reaction module for multienzyme cascades. *Chem Synth* 2023;3:49. <https://dx.doi.org/10.20517/cs.2023.40>

**Received:** 14 Aug 2023 **First Decision:** 13 Oct 2023 **Revised:** 27 Oct 2023 **Accepted:** 17 Nov 2023 **Published:** 27 Nov 2023

**Academic Editor:** Ying Wan **Copy Editor:** Yanbing Bai **Production Editor:** Yanbing Bai

## Abstract

Enzymatic alcohol oxidation (EAO) is highly attractive thanks to its efficiency, selectivity, and sustainability benefits, but it is often neglected as a catalytic tool for practical production due to the instability and non-reusability of enzymes. Herein, a non-enantioselective alcohol dehydrogenase engineered from *Candida parapsilosis* (CpsADH) and a laccase from *Trametes versicolor* was immobilized on mesoporous silica nanoflowers (MSNs), fabricating CpsADH@MSNs (41 U/g<sub>support</sub>) and laccase@MSNs (67 U/g<sub>support</sub>) for EAO, respectively. The structural and functional properties of the MSNs endowed the immobilized enzymes with higher stability than free enzymes, and the relative activity of the immobilized enzyme was 52% and 63%, respectively, after being reused five times. The immobilized enzymes exhibited high activity, selectivity, and complementary substrate specificity in alcohol oxidation. The optimized EAO, as a versatile cascade module, was coupled with several other enzymatic transformations for multi-enzymatic synthesis of high value-added chemicals. The chiral alcohols and amines were produced with 99% ee and 84% to 98% ee, respectively, and (*R*)-benzoin and 2-furoic acid were prepared with 91% yield, 99% ee and 86% yield, respectively, demonstrating the synthetic utility of the immobilized enzymes.

**Keywords:** Alcohol oxidation, asymmetric synthesis, enzyme immobilization, multienzyme cascades, mesoporous silica nanoflowers



© The Author(s) 2023. **Open Access** This article is licensed under a Creative Commons Attribution 4.0 International License (<https://creativecommons.org/licenses/by/4.0/>), which permits unrestricted use, sharing, adaptation, distribution and reproduction in any medium or format, for any purpose, even commercially, as long as you give appropriate credit to the original author(s) and the source, provide a link to the Creative Commons license, and indicate if changes were made.



## INTRODUCTION

Selective oxidation of alcohols to corresponding carbonyl compounds, such as aldehydes, ketones, and carboxylic acids, has become one of the most important chemical transformations in organic chemistry and chemical industries<sup>[1]</sup>. Various approaches have been developed for this fundamental reaction. Conventional methods typically required stoichiometric toxic oxidants such as sodium hypochlorite, potassium permanganate, potassium dichromate, and organic peroxides<sup>[2-4]</sup>, resulting in high cost and environmental problems<sup>[5-7]</sup>. Nowadays, catalytic oxidation approaches enable the utilization of environmentally more acceptable oxidants such as molecular oxygen (O<sub>2</sub>). Among them, metal-catalyzed aerobic oxidation of alcohols has attracted considerable attention<sup>[8-13]</sup>. Particularly, the heterogeneous catalysis is more preferred by industrial production due to its advantages of high recyclability, low toxicity, and simple protocol<sup>[14-16]</sup>. Although significant improvements have been made, the metal-catalyzed systems usually suffer from harsh reaction conditions (high temperatures and volatile organic solvents), metal residues, and low selectivity. In addition, O<sub>2</sub> cannot be used on a large scale due to the tendency to form explosive mixtures. Therefore, it is still a critical task to develop metal-free catalytic systems for the green, mild, selective, and safe oxidation of alcohols.

From an environmental and safety perspective, enzymatic alcohol oxidation (EAO) is more attractive due to its mild reaction conditions, high selectivity, and eco-friendliness<sup>[17]</sup>. Various enzymes are capable of supporting this task, for instance, the most widely used alcohol dehydrogenases (ADHs), which utilize the oxidized nicotinamide cofactor [NAD(P)<sup>+</sup>] as a hydride acceptor<sup>[18]</sup>. Although the complete oxidation of primary alcohols to aldehydes by ADHs has been extensively explored<sup>[19]</sup>, the similar transformation from racemic secondary alcohols towards prochiral ketones is generally problematic because only one of the enantiomers can be oxidized. To solve this issue, two enantiocomplementary ADHs are usually applied<sup>[20]</sup>, albeit with a more complicated reaction scheme. Non-enantioselective ADHs are ideal biocatalysts for the complete oxidation of racemic alcohols but remain highly scarce. Recently, a non-enantioselective ADH engineered from *Candida parapsilosis* (CpsADH) with high specificity toward secondary benzyl alcohols has been reported<sup>[20]</sup>. Besides ADHs, complete oxidation of racemic *sec*-alcohols (e.g., activated benzylic, allylic, and propargylic alcohols) by laccase has also been reported, where the organocatalyst 2,2',6,6'-tetramethylpiperidine-N-oxyl (TEMPO) is commonly used as the oxidant<sup>[21-24]</sup>, although it is generally reported to selectively oxidize primary alcohols. In addition, EAO has proven to be a versatile cascade module that can be coupled with a broad of enzymatic transformations for multi-enzymatic production of high-value chemicals<sup>[25]</sup>. Despite this, enzymes are often neglected as catalytic tools for practical production due to their instability and non-reusability<sup>[26,27]</sup>.

Immobilization of enzymes on suitable support has been proven to be effective in improving their stability, reusability, and even activity<sup>[28-30]</sup>. The nature of the support materials has a significant influence on the catalytic performance of enzymes. Mesoporous silica materials have emerged as an attractive immobilization platform due to their distinct structural and functional properties, including high surface area, high stability, high pore accessibility, high permeability, high biocompatibility, and easily functionalized groups<sup>[28,31,32]</sup>. Particularly, mesoporous silica nanoflowers (MSNs) have demonstrated superiority in immobilizing various enzymes such as lipases<sup>[33,34]</sup>, transaminases<sup>[35]</sup>, and ene-reductases<sup>[36,37]</sup>. However, to the best of our knowledge, MSN-based immobilized enzymes for alcohol oxidation have not been reported yet. Herein, we have fabricated two MSN-based immobilized enzymes, i.e., the non-enantioselective CpsADH (CpsADH@MSNs) and laccase (laccase@MSNs), for the efficient and complete oxidation of racemic alcohols. Compared to free enzymes, MSN-based biocatalysts achieved significant improvements in pH, thermal, mechanical, and storage stability. The CpsADH@MSNs exhibited high activity and specificity toward *sec*-alcohols, while the laccase@MSNs showed high catalytic performance in

the full oxidation of both *prim*- and *sec*-alcohols. The synthetic utility of the immobilized enzymes and the EAO was demonstrated in several multienzyme cascades for the synthesis of high value-added synthons.

## EXPERIMENTAL

### Materials

Tetraethyl orthosilicate (TEOS), sodium acetate, ethanol, glutaraldehyde (GA), cyclohexane, *n*-butyl alcohol, and urea of analytical grade were purchased from Tianjin Chemical. Additionally, 2,2'-Azinobis-(3-ethylbenzthiazoline-6-sulphonate) (ABTS) and CTAB (cetyltrimethylammonium bromide) were purchased from Aldrich-sigma. Laccase from *Trametes versicolor* was also obtained from Sigma-Aldrich. Moreover, (3-aminopropyl) triethoxysilane (APTES) was purchased from Alfa Aesar Chemical Co., Ltd (Tianjin, China). Furthermore, 1-Phenylethanol and benzyl alcohol were purchased from Aladdin Biochemical Technology Co., Ltd. (Shanghai, China). All chemicals were used as received without further purification.

### Preparation of CpsADH@MSNs and laccase@MSNs

For *CpsADH* immobilization, 50 mg of MSNs activated under different conditions were uniformly dispersed in 5 mL PBS (50 mM, pH = 8.5) by ultrasound for 30 min. Then, 5 mL of *CpsADH* solution (1.2–11.5 mg<sub>protein</sub>/mL) was added, and the mixture was shaken at 170 rpm for different times to explore the optimum GA concentration, covalent bonding time, immobilized time, and *CpsADH* concentration. The immobilized *CpsADH* (*CpsADH*@MSNs) was washed with PBS (50 mM, pH = 8.5) three times to ensure the covalent binding of *CpsADH* on MSNs. The protein content was determined by the Bradford method.

For laccase immobilization, 50 mg of MSNs activated under different conditions were uniformly dispersed in 5 mL acetate buffer solution (pH = 4.5, 0.1 M) by ultrasound for 30 min. Then, 5 mL of laccase solution (2–16 mg<sub>enzyme powder</sub>/mL) was added, and the mixture was shaken at 170 rpm for different times to explore the optimum GA concentration, covalent bonding time immobilized time, and laccase concentration.

### Oxidation of alcohols by CpsADH@MSNs or laccase@MSNs

The oxidation of alcohols (20 mM) by *CpsADH*@MSNs (10 mg) was performed in 1 mL PBS buffer (50 mM, pH = 8.5) containing NAD<sup>+</sup> (0.2 mM) and acetone (200 mM). After the reaction at 40 °C and 180 rpm for 6 h, the catalyst was separated by centrifugation; the reaction product was extracted by ethyl acetate, and the organic phase was dried with anhydrous Na<sub>2</sub>SO<sub>4</sub>. The solvent was concentrated in a vacuum to obtain crude products. The product was purified by column chromatography (petroleum ether/ethyl acetate = 8/1, v/v).

The oxidation of alcohols (20 mM) by laccase@MSNs (10 mg) was performed with laccase@MSNs in 1 mL acetate buffer solution (100 mM, pH = 4.5) containing TEMPO (12 mM). After the reaction at 40 °C and 180 rpm for 24 h, the catalyst was separated by centrifugation, the reaction product was extracted by ethyl acetate, and the organic phase was dried with anhydrous Na<sub>2</sub>SO<sub>4</sub>. The solvent was concentrated in a vacuum to obtain crude products. The product was purified by column chromatography (petroleum ether/ethyl acetate = 8/1, v/v).

### Bienzymatic deracemization of alcohols

The substrate (20 mM) was oxidized with *CpsADH*@MSNs (10 mg) in 1 mL PBS buffer (50 mM, pH = 8.5) containing NAD<sup>+</sup> (0.2 mM) and acetone (200 mM). After the reaction at 40 °C and 180 rpm for 12 h, the catalyst was separated by centrifugation. The acetone was removed by heating at 60 °C, and the pH was adjusted to 9.5. Then 1 mL ADH-A (from *Rhodococcus ruber*)<sup>[38]</sup> solution and isopropanol (30% v/v) were added. After the reaction at 30 °C for 24 h, the reaction solution was extracted by ethyl acetate the reaction

solution was extracted by ethyl acetate. The yields and ee values were calculated by gas chromatography.

### Bienzymatic hydrogen-borrowing alcohol amination

The substrate (20 mM),  $\text{NAD}^+$  (0.2 mM), *CpsADH*@MSNs (10 mg) were added to the 5 mL round-bottomed flask containing 1 mL  $\text{NH}_4\text{Cl}/\text{NH}_4\text{OH}$  buffer (2 M, pH = 9.0) and 10  $\mu\text{L}$  DMSO. Subsequently, 1 mL *Ja*-AmDH (from *Jeotgalicoccus aerolatus*)<sup>[39]</sup> crude enzyme solution was added. The mixture was stirred at 30 °C for 48 h. After the reaction was complete, the catalyst was separated by centrifugation. The product was extracted with diethyl ether (5 mL), and the organic phase was dried with anhydrous  $\text{Na}_2\text{SO}_4$ . The solvent was concentrated in a vacuum to obtain a crude product. The product was purified by column chromatography (ethyl acetate/methanol = 99/1, v/v).

### Bienzymatic carboligation

Benzyl alcohol (20 mM) was oxidized with laccase@MSNs (10 mg) in 1 mL sodium acetate buffer (100 mM, pH = 4.5) containing TEMPO (12 mM). After the reaction at 40 °C and 180 rpm for 24 h, the catalyst was separated by centrifugation. Then, pH was adjusted to 7.5 with hydrochloric acid, and  $\text{MgSO}_4$  (2.5 mM), ThDP (0.15 mM), and 1 mL of benzaldehyde lyase (BAL) (from *Pseudomonas fluorescens* Biovar I)<sup>[40]</sup> solution were added. After the reaction at 30 °C for 24 h, the reaction solution was extracted by ethyl acetate, and the organic phase was dried with anhydrous  $\text{Na}_2\text{SO}_4$ . The solvent was concentrated in a vacuum to obtain a crude product. The product was purified by column chromatography (petroleum ether/ethyl acetate = 5/1, v/v).

### Biocatalytic relay oxidation

Furfuryl alcohol (20 mM) was oxidized with laccase@MSNs (10 mg) in 1 mL sodium acetate buffer (100 mM, pH = 4.5) containing TEMPO (12 mM). After the reaction at 40 °C and 180 rpm for 24 h, the catalyst was separated by centrifugation, and the pH of the reaction solution was adjusted to 7. Then, 14 mg of whole cell catalysts (dry weight) over-expressing horse liver ADH (HLADH) (from *Equus caballus*)<sup>[41]</sup> were added. After the reaction at 30 °C for 96 h, the reaction solution was extracted by ethyl acetate, and the organic phase was dried with anhydrous  $\text{Na}_2\text{SO}_4$ . The solvent was concentrated in a vacuum to obtain a crude product. The product was purified by column chromatography (petroleum ether/ethyl acetate = 2/1, v/v).

## RESULTS AND DISCUSSION

### Preparation and characterization of the immobilized enzymes

Wrinkled MSNs were prepared by a modified reverse microemulsion method<sup>[38]</sup> and then functionalized with an amino ( $-\text{NH}_2$ ) group, providing reaction sites for covalent immobilization of enzymes. The morphology and pore structures of the MSNs were characterized by SEM and TEM. As shown in [Supplementary Figure 1A](#), the MSNs were flower-like nanospheres with an average diameter of 390 nm, and they have a large specific surface area due to their small size and surface folds. The TEM images of the MSNs demonstrated the distinctive fibrous center-radial channels [[Supplementary Figure 1B](#)], which can facilitate the mass transfer. The specific surface area and pore diameter were calculated based on  $\text{N}_2$  adsorption-desorption isotherms and pore size distributions [[Supplementary Figure 2](#)], which are 543.08  $\text{m}^2/\text{g}$  and 14.58 nm, respectively, corresponding to the results of electron microscopy. The large specific surface area of MSNs supplies enough sites for the enzymes to covalently bond, and the mesoporous channels ensure smooth entering of the enzymes, and they synergistically enhance the immobilization efficiency of the enzyme.

Although the enzymes for complete oxidation of *sec*-alcohols, especially benzyl alcohols to ketones, are highly constrained, non-enantioselective *Cps*ADH and laccase have been reported to achieve this goal and were, therefore, chosen as the model enzymes. The enzymes were covalently bound to the MSNs using GA as a crosslinking agent. Immobilized enzymes were prepared using FITC-labeled *Cps*ADH and Rhodamine B-labeled laccase for the confocal laser scanning microscope (CLSM) analysis. The green fluorescence of immobilized *Cps*ADH [Figure 1A] and the red fluorescence of immobilized laccase [Figure 1B] can be clearly observed, evidencing the successful immobilization of the enzymes. In FT-IR spectra, a strong band at  $1,630\text{ cm}^{-1}$  appeared, which was attributed to the presence of the C=N bond formed between GA and enzymes [Figure 1C]. In addition, the absorption peaks at  $1,394$  and  $1,540\text{ cm}^{-1}$  were assigned to the stretching vibration of C-N bonds and N-H bending vibration, respectively<sup>[42-44]</sup>. These results further confirmed the successful enzyme immobilization.

The effectiveness of enzyme immobilization was dependent on the GA concentration, covalent bonding time, enzyme concentration, and immobilization time. The relationship between the relative enzyme activity and GA concentration was shown in Figure 2A and B. With the increase of GA concentration, the relative activities of *Cps*ADH@MSNs and laccase@MSNs increased gradually due to the greater immobilization of enzyme molecules on the support by formation of Schiff bases between GA and enzymes<sup>[45,46]</sup>. However, too high GA concentrations also caused decreased relative enzyme activity because the excess GA caused enzyme conformation change and enzyme self-crosslinking, which led to a steric hindrance effect on enzyme immobilization<sup>[47,48]</sup>. The maximum relative activity of *Cps*ADH@MSNs and laccase@MSNs were obtained with the use of 3 wt% and 5 wt% GA, respectively.

The crosslinking time of GA and MSNs also has a significant effect on immobilization efficiency. As depicted in Figure 2C and D, the optimal activity of *Cps*ADH@MSNs and laccase@MSNs were obtained after crosslinking for 3 h and 4 h, respectively. With the increase of covalent bonding time, the enzyme attachment sites on the nanoparticles increased, resulting in an increase in the amount of protein fixation and the activity of immobilized enzymes. The spatial grid structure of the support increased over time, restricting the access of more enzyme molecules<sup>[49]</sup>. Hence, an appropriate covalent bonding time was essential to maintain high enzyme activity. The effects of immobilization time and enzyme concentration on the relative activity of immobilized enzymes were shown in Figure 3A-D. With the increase of fixation time and enzyme concentration, the specific enzyme activity and protein load of the fixed enzyme tended to be stable. As shown in Supplementary Figure 3A, the immobilization yield and enzyme activity recovery of *Cps*ADH@MSNs were measured. The enzyme activity recovery of *Cps*ADH@MSNs decreased gradually with the increase of protein concentration, and the immobilization yield reached the maximum of 47.9% at 3 mg/mL. However, since the protein content of the laccase powder used was too low to accurately measure the immobilization yield, only the recovery of enzyme activity from laccase immobilization was tested. The enzyme activity recovery of laccase@MSNs peaked at 27.8% at 6 mg/mL [Supplementary Figure 3B]. With the immobilization time increasing to a certain extent, the activity of immobilized enzymes increases slowly, which may be due to the nearing saturation of enzyme immobilization or the insufficient enzyme concentration to support the enzyme immobilization. The value of the protein fixation amount and the immobilized enzyme activity kept rising with the increasing enzyme concentration until reaching supporter saturation<sup>[30]</sup>.

### Enzymatic properties of free and immobilized enzymes

A series of parameters, such as temperature, pH, storage time, and numbers for recycling, were studied to evaluate the stability of the immobilized enzymes. Both the free *Cps*ADH and *Cps*ADH@MSNs showed the optimal activity at  $30\text{ }^{\circ}\text{C}$  [Figure 4A]. The activity of free *Cps*ADH decreased significantly no matter whether the temperature was below nor above  $30\text{ }^{\circ}\text{C}$ , while the *Cps*ADH@MSNs exhibited high stability in a



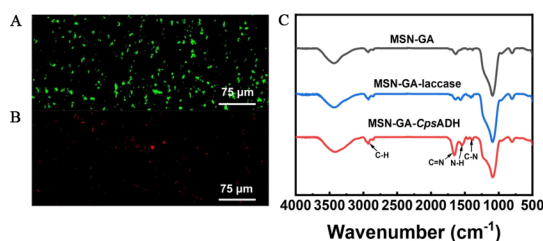


**Figure 1.** CLSM images of CpsADH@MSNs (A) and laccase@MSNs (B); Fourier transform infrared spectroscopy (FT-IR) spectra of MSNs-GA, CpsADH@MSNs, and laccase@MSNs (C).

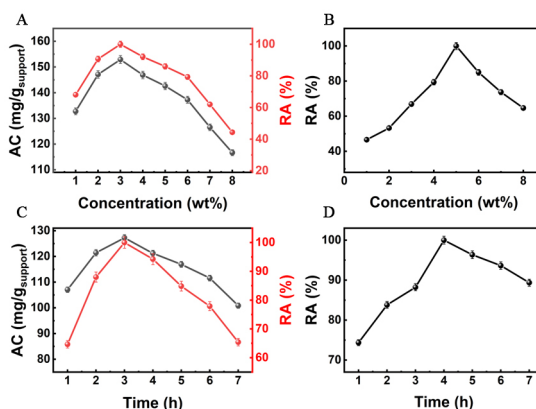


**Figure 2.** Effects of GA concentration on the relative activity (RA) of immobilized enzyme and adsorption capacity (AC) of MSNs: CpsADH@MSNs (A); laccase@MSNs (B); Effects of covalent bonding time on the relative activity (RA) of immobilized enzyme and adsorption capacity (AC) of MSNs: CpsADH@MSNs (C); laccase@MSNs (D).

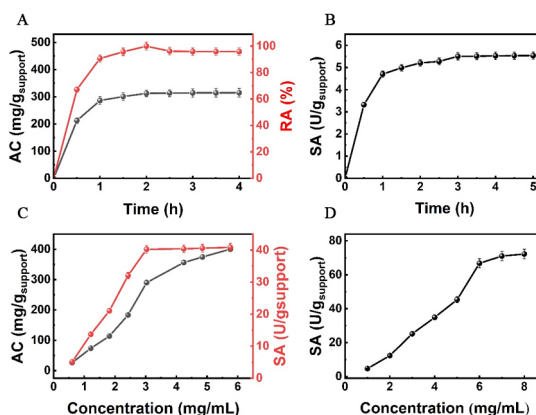


**Figure 3.** Effects of immobilization time on the specific activity (SA) and relative activity (RA) of immobilized enzyme and adsorption capacity (AC) of MSNs: CpsADH@MSNs (A); laccase@MSNs (B); Effects of protein concentration on the specific activity (SA) and relative activity (RA) of immobilized enzyme and adsorption capacity (AC) of MSNs: CpsADH@MSNs (C); laccase@MSNs (D).

wide temperature range. Free CpsADH and CpsADH@MSNs showed the highest activity at pH = 8.5 [Figure 4B]. When the pH value was below or above 8.5, the activity of free CpsADH decreased significantly, while the CpsADH@MSNs showed high stability in a wide pH range. The optimum temperature and pH of free and immobilized laccase were confirmed to be 45 °C and 4.5, respectively. Similarly, the laccase@MSNs also exhibited higher stability than the free laccase [Figure 4C and D].

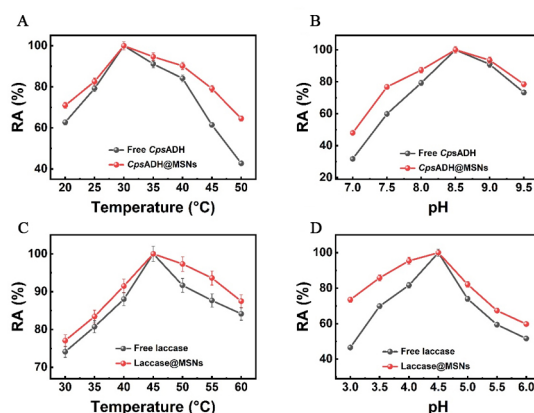


**Figure 4.** Optimal temperature of free *CpsADH* and *CpsADH*@MSNs (A); and free laccase and laccase@MSNs (C); Optimal pH of free *CpsADH* and *CpsADH*@MSNs (B); and free laccase and laccase@MSNs (D).

We also investigated the activity variation of free and immobilized enzymes after the incubation at 30 °C [Figure 5A and B] and 50 °C [Figure 5C and D] for a period of time. After four days of incubation at 30 °C, the relative enzyme activity of the *CpsADH*@MSNs remained at 46%, while only < 10% for the free *CpsADH*. After incubation at 50 °C for 100 min, the relative activity of the *CpsADH*@MSNs and free *CpsADH* were 54% and 35%, respectively. The relative enzyme activity of laccase@MSNs was > 70% after one week of heat preservation at 30 °C, and its relative enzyme activity was 58% after 5 h of heat preservation at 50 °C, which was higher than that of the free laccase. To investigate the pH stability of immobilized enzymes, free *CpsADH* and *CpsADH*@MSNs were incubated in citrate buffer solution (0.1 M, pH = 4) and phosphate buffer solution (50 mM, pH = 9.5) for 3.5 h, and the relative activity of *CpsADH*@MSNs was 61% and 68%, respectively [Figure 6A]. The free laccase and laccase@MSNs were incubated for 10 h in a 50 mM phosphate buffer solution with pH = 2 and 9, and the relative activity of laccase@MSNs was 85% and 72%, respectively [Figure 6B]. These results confirmed the high pH stability of the immobilized enzymes. However, the free *CpsADH* and free laccase are more sensitive to extreme pH conditions. As shown in [Figure 6C and D], the *CpsADH*@MSNs and laccase@MSNs also have higher long-term storage stability (stored at 4 °C) than the free enzymes. The better stability of the immobilized enzyme may be due to the multi-point interaction between the enzyme and the nanoparticle, which stabilizes the weak force within the molecule and prevents the enzyme from denaturation or inactivation<sup>[50,51]</sup>.

### Catalytic performance of the immobilized enzymes

Having obtained and characterized the *CpsADH*@MSNs and laccase@MSNs, we turned our attention to investigating their catalytic performance using 1-phenylethanol as a model substrate. After the optimization of reaction conditions, pH = 8.5 and 40 °C were selected to be the optimal condition for *CpsADH*@MSNs [Supplementary Table 1], and pH = 4.5 and 40 °C were optimal for laccase@MSNs [Supplementary Table 2]. The appropriate temperature and pH are important components of the reaction. At lower temperatures, the structure of the enzymes is affected. When the temperature is lower, the reaction rate of the enzyme will also slow down because the low temperature will reduce the transfer rate of the enzyme molecules and the substrates. When the temperature is too high, the enzyme will be denatured and deactivated due to structural changes. Similarly, various pH values will also change the molecular structures of the enzymes, which further affects their activity<sup>[52,53]</sup>.

In a *CpsADH*@MSN catalytic system, a co-substrate method was applied to achieve cofactor regeneration, which is important for improving economic benefit. Using acetone as a co-substrate, the dosage of the

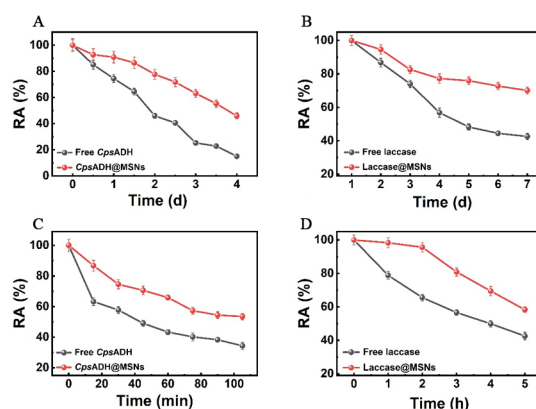


**Figure 5.** Thermal stability of the free enzyme and immobilized enzyme at 30 °C: *CpsADH*@MSNs (A); laccase@MSNs (B); Thermal stability of the free enzyme and immobilized enzyme at 50 °C: *CpsADH*@MSNs (C); laccase@MSNs (D).

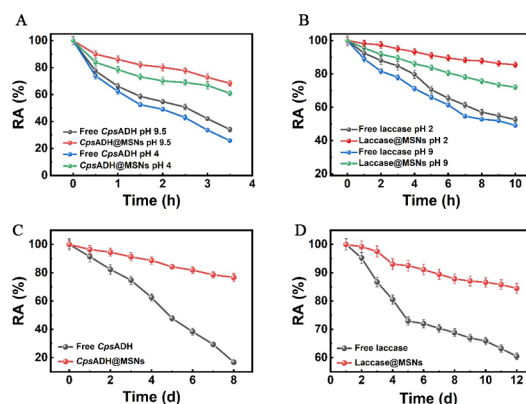


**Figure 6.** The stability of free and immobilized enzymes at pH = 2 and pH = 9: *CpsADH*@MSNs (A); laccase@MSNs (B); long-term storage stability of free and immobilized enzymes: *CpsADH*@MSNs (C); laccase@MSNs (D).

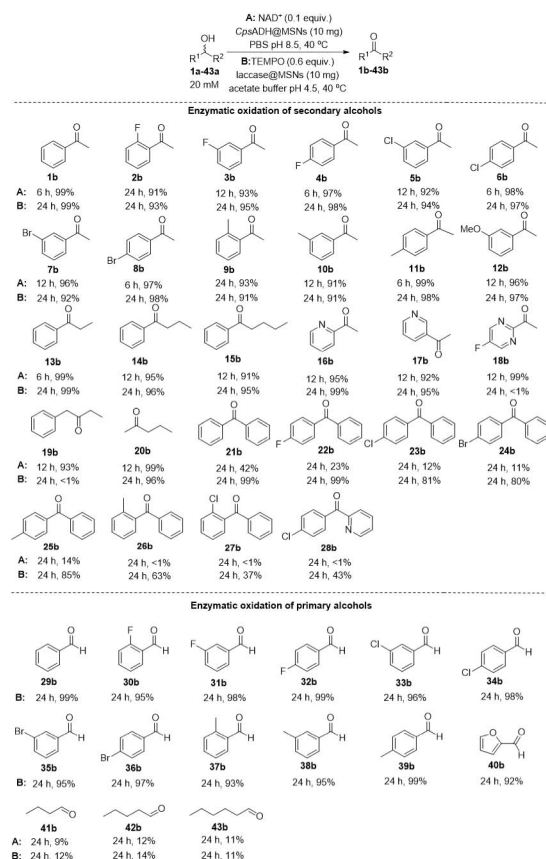
cofactor ( $\text{NAD}^+$ ) could be reduced to 0.01 equivalent, and the reaction conversion was still up to 99%, albeit with increased reaction time [Supplementary Table 1, Entries 6-9]. According to the literature<sup>[54]</sup>, the catalytic mechanism of laccase/TEMPO systems was proposed. First, laccase oxidizes the stable oxyl-radical form of TEMPO to the oxoammonium ion (the actual oxidant species), which can oxidize the alcohol to ketone (or aldehyde) through a hydrogen abstraction process while generating hydroxylamine (TEMP-OH). The generated TEMP-OH was then re-oxidized to TEMPO radical. Theoretically, only a catalytic amount of TEMPO can support this transformation, which was confirmed by experimental results. However, a low amount of TEMPO led to an extremely low reaction rate. For example, only 24% conversion was obtained after reacting 24 h if only using 0.2 equivalent of TEMPO. Increasing to TEMPO equivalent to 0.6, the conversion increased to 99% during the same reaction time [Supplementary Table 2, Entries 1-3]. Higher substrate concentrations were also tested for these two immobilized enzymes. The complete conversion can still be obtained by *CpsADH*@MSNs after reacting 36 h with a 100 mM scale, and laccase@MSNs gave 91% conversion after reacting four days with a 200 mM scale. We then examined the operational stability of the *CpsADH*@MSNs and laccase@MSNs using the catalytic oxidation of 1-phenylethanol as the model reaction. As shown in Supplementary Figure 4, *CpsADH*@MSNs still have good catalytic performance with relative activity of 52% after five cycles, and laccase@MSNs maintained 63% relative activity after five cycles. These results highlighted the potential of the immobilized enzymes for practical applications. Due to the fact that



only negligible enzyme leakage (0.5% for *Cps*ADH@MSNs) was detected after five reuse cycles [Supplementary Figure 5], the decreased activity of the immobilized enzymes was presumed to be an enzyme inactivation during the reaction process.

To demonstrate the general applicability of the immobilized enzymes, we explored their substrate scope under the optimized reaction conditions. As shown in Scheme 1, the substrate portfolio could be expanded to both electron-deficient and electron-rich secondary alcohols, and all gave high yields (91%-99%). In a *Cps*ADH@MSNs catalytic system, a substituent effect of substrates on reaction rates was observed, but this phenomenon was not found for laccase@MSNs. Generally, the reaction rates of the *ortho*-, *meta*-, and the *para*-substituted substrates increased in turn. For example, the complete oxidation of *ortho*-, *meta*-, and the *para*-substituted alcohols required 24, 12, and 6 h, respectively. Both the *Cps*ADH@MSNs and laccase@MSNs showed high activity and selectivity toward (hetero)aryl-alkyl alcohols (**1-19b**) and alkyl-alkyl alcohol (**20b**), except for laccase@MSNs towards **18b** and **19b**. No obvious substrate/product inhibition was found, and other reasons for the low activity of laccase@MSNs towards these two compounds are not clear. Laccase@MSNs also exhibited high activity in the oxidation of aryl alcohols (**21-27b**), while *Cps*ADH@MSNs displayed only low activity toward aryl alcohols. Similarly, a substituent effect of substrates on yield was also observed. The yields of the *ortho*-substituted substrates were lower than those of the *para*-substituted substrates. An obvious decrease in enzyme activity toward aryl heteroaryl alcohol (**28b**) was also found. In addition, the laccase@MSNs exhibited high catalytic activity toward primary aromatic alcohols (**29-40b**) but low activity toward primary aliphatic alcohols (**41-43b**). The *Cps*ADH@MSNs not only failed to oxidize primary aromatic alcohols but also exhibited low activity toward primary aliphatic alcohols due to their high substrate specificity. Notably, no overoxidized by-products were observed for both the immobilized enzymes, demonstrating high chemo-selectivity. To demonstrate the synthetic application of the immobilized enzymes, gram-scale reactions were also performed using 1-phenylethanol as a model substrate. The *Cps*ADH@MSNs and laccase@MSNs could convert 1.06 g substrates (350 mM, 25 mL) to the desired ketone in 94% [Supplementary Table 1, Entry 16] and 89% yield [Supplementary Table 2, Entry 14], respectively. Although the alcohol oxidation has been extensively studied, the existing methods generally required strong oxidizing agents and metal catalysts and suffered from harsh reaction conditions, including high reaction temperatures and organic solvents [Supplementary Table 3]. In contrast, the immobilized enzymes enable the alcohol oxidation under mild conditions through metal-free catalytic systems without the use of strong oxidizing agents, making it a green, mild, and safe approach. However, from the point of view of industrial applications, more efforts should be made to shorten the reaction time and increase the substrate loading.

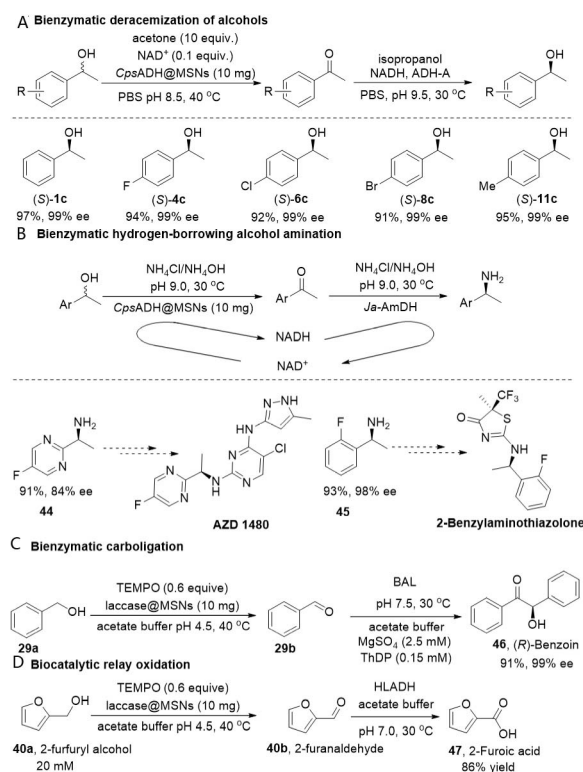
To further demonstrate the synthetic utility of the EAO, we investigated its application in multienzyme cascades for the enantioselective synthesis of high value-added synthons, such as chiral alcohols and amines<sup>[17]</sup>. The conversion of racemic alcohols to enantiopure alcohols and amines is of great importance in pharmaceutical manufacturing<sup>[55]</sup> because racemic alcohols are commercially available and easily accessible, and these enantiopure compounds are often useful and valuable pharmaceutical intermediates. Coupling non-enantioselective alcohol oxidation with highly enantioselective ketone reduction, an oxidation-reduction cascade can be successfully constructed to achieve deracemization of alcohols, converting racemic alcohols to their enantiopure counterparts<sup>[56,57]</sup>. By combining *Cps*ADH@MSNs with ADH-A, a series of enantiopure  $\alpha$ -benzyl alcohols were obtained in 91%-97% yields and 98%-99% ee from racemic alcohols [Scheme 2A]. The redox-neutral hydrogen-borrowing cascade catalyzed by ADHs and amine dehydrogenases (AmDHs) has become an elegant approach for synthesizing chiral amines from racemic alcohols, in which the ADH-catalyzed alcohol oxidation is accompanied by the consumption of NADH and generation of NAD<sup>+</sup>, while the AmDH-catalyzed ketone reductive amination leads to the conversion of



**Scheme 1.** The enzymatic oxidation of alcohol by the CpsADH@MSNs and laccase@MSNs.

NAD<sup>+</sup> to NADH, creating a cofactor self-regeneration system<sup>[58,59]</sup>. Combining CpsADH@MSNs with an engineered *Ja*-AmDH, two pharmaceutically relevant chiral  $\alpha$ -aryl primary amines were synthesized in high yields and enantioselectivity [Scheme 2B].

Enantioselective C-C bond-forming reactions have become a powerful tool for the synthesis of enantiopure compounds from readily available non-chiral substrates, such as the benzoin reaction. In this regard, a bienzymatic cascade combining laccase@MSNs and BAL was developed for the enantioselective synthesis of (*R*)-benzoin from benzyl alcohol in 91% yield and 99% ee via C-C bond formation [Scheme 2C]. Upgrading furfuryl alcohols to furancarboxylic acids is of great significance for biomass conversion and high value-added downstream chemical synthesis. A biocatalytic relay oxidation approach was developed for oxidizing furfuryl alcohol to furoic acids, a versatile raw material used for producing various pharmaceutical, agricultural, and industrial chemicals. Furfuryl alcohol was first oxidized to furanaldehyde by laccase@MSNs and then further oxidized to furoic acid by recombinant whole-cells overexpressing HLADH<sup>[41]</sup>, with an overall yield of 86% [Scheme 2D]. The alcohol oxidation of immobilized enzyme developed in this work, as a general module of multienzyme cascade reaction, successfully prepared a variety of high value-added chiral compounds with multienzyme cascade, proving the feasibility of this general module. Because of the wide range of applicable substrates and the diversity of multienzyme cascades, this module has a broad application prospect.



Scheme 2. Multienzyme cascades for the synthesis of high value-added compounds.

## CONCLUSIONS

In conclusion, the immobilization of *CpsADH* and laccase on MSNs was achieved for EAO. The specific enzyme activities of the optimized *CpsADH*@MSNs and laccase@MSNs were 41 and 67 U/g<sub>support</sub>, respectively. The immobilized enzymes showed higher stability than the free enzymes and exhibited high catalytic activity and selectivity in oxidation of various alcohols under mild conditions. As a versatile cascade module, the EAO was coupled with several other enzymatic transformations, achieving multienzyme cascades for alcohol deracemization, hydrogen-borrowing alcohol amination, enantioselective C-C bond formation, and relay oxidation of biomass-derived furfuryl alcohol. This work highlighted the application potential of the immobilized enzymes and EAO in synthetic chemistry.

## DECLARATIONS

### Acknowledgments

We sincerely thank all the team members who participated in this study.

### Authors' contributions

Carried out the catalyst preparation, characterization, and catalytic tests and prepared the draft manuscript: Fu K

Carried out the MSN preparation: Dong L, Liu P

Performed the TEM, SEM, and FT-IR characterization: Zhou L, Liu G, Gao J, Gao B

Planned the study, analyzed the data, and wrote the manuscript: Liu Y, Jiang Y

### Availability of data and materials

Supplementary Materials are available online for this paper, and the data supporting the findings of this study are available within its supplementary materials.

### Financial support and sponsorship

This research was supported by the National Key Research and Development Program of China (2021YFC2104100); The National Natural Science Foundation of China (22378096, 22078081, and 22178083); The Natural Science Foundation of Hebei Province (B2022202014 and B2020202021); The S&T Program of Hebei (21372805D, 21372804D, and 20372802D); The Natural Science Foundation of Tianjin (20JCYBJC00530); And the Science Technology Research Project of Higher Education of Hebei Province (QN2021045).

### Conflicts of interest

All authors declared that there are no conflicts of interest.

### Ethical approval and consent to participate

Not applicable.

### Consent for publication

Not applicable.

### Copyright

© The Author(s) 2024.

## REFERENCES

1. Asthana M, Syiemlieh I, Kumar A, Lal RA. Direct oxidation of alcohols catalysed by heterometallic complex  $[\text{CuNi}(\text{bz})_3(\text{bpy})_2] \text{ClO}_4$  to aldehydes and ketones mediated by hydrogen peroxide as a terminal oxidant. *Inorganica Chimica Acta* 2020;502:119286. DOI
2. Shaabani A, Shaabani S, Afaridoun H. Highly selective aerobic oxidation of alkyl arenes and alcohols: cobalt supported on natural hydroxyapatite nanocrystals. *RSC Adv* 2016;6:48396-404. DOI
3. Mallat T, Baiker A. Oxidation of alcohols with molecular oxygen on solid catalysts. *Chem Rev* 2004;104:3037-58. DOI PubMed
4. Nakagawa K, Konaka R, Nakata T. Oxidation with Nickel Peroxide. I. oxidation of alcohols. *J Org Chem* 1962;27:1597-601. DOI
5. Lou JD, Xu ZN. Selective oxidation of primary alcohols with chromium trioxide under solvent free conditions. *Tetrahedron Lett* 2002;43:6095-7. DOI
6. Uyanik M, Ishihara K. Hypervalent iodine-mediated oxidation of alcohols. *Chem Comm* 2009:2086-99. DOI PubMed
7. Taylor RJ, Reid M, Foot J, Raw SA. Tandem oxidation processes using manganese dioxide: discovery, applications, and current studies. *Acc Chem Res* 2005;38:851-69. DOI PubMed
8. Hasanpour B, Jafarpour M, Feizpour F, Rezaeifard A. Copper(II)-ethanolamine triazine complex on chitosan-functionalized nanomagnetite for catalytic aerobic oxidation of benzylic alcohols. *Catal Lett* 2021;151:45-55. DOI
9. Martín SE, Suárez DF. Catalytic aerobic oxidation of alcohols by  $\text{Fe}(\text{NO}_3)_3\text{-FeBr}_3$ . *Tetrahedron Lett* 2002;43:4475-9. DOI
10. Qiu S, Li Y, Xu H, et al. Efficient catalytic oxidation of benzyl alcohol by tetrasubstituted cobalt phthalocyanine-MWCNTs composites. *Solid State Sci* 2022;129:106905. DOI
11. Schultz MJ, Hamilton SS, Jensen DR, Sigman MS. Development and comparison of the substrate scope of Pd-catalysts for the aerobic oxidation of alcohols. *J Org Chem* 2005;70:3343-52. DOI PubMed PMC
12. Personick ML, Zugic B, Biener MM, Biener J, Madix RJ, Friend CM. Ozone-activated nanoporous gold: a stable and storable material for catalytic oxidation. *ACS Catal* 2015;5:4237-41. DOI
13. Parmeggiani C, Cardona F. Transition metal based catalysts in the aerobic oxidation of alcohols. *Green Chem* 2012;14:547-64. DOI
14. Polshettiwar V, Varma RS. Green chemistry by nano-catalysis. *Green Chem* 2010;12:743-54. DOI
15. Shibuya M, Tomizawa M, Suzuki I, Iwabuchi Y. 2-azaadamantane N-oxyl (AZADO) and 1-Me-AZADO: highly efficient organocatalysts for oxidation of alcohols. *J Am Chem Soc* 2006;128:8412-3. DOI PubMed
16. Punniyamurthy T, Velusamy S, Iqbal J. Recent advances in transition metal catalyzed oxidation of organic substrates with molecular oxygen. *Chem Rev* 2005;105:2329-63. DOI PubMed
17. Liu J, Wu S, Li Z. Recent advances in enzymatic oxidation of alcohols. *Curr Opin Chem Biol* 2018;43:77-86. DOI
18. Moa S, Himo F. Quantum chemical study of mechanism and stereoselectivity of secondary alcohol dehydrogenase. *J Inorg Biochem* 2017;175:259-66. DOI PubMed
19. Kroutil W, Mang H, Edegger K, Faber K. Biocatalytic oxidation of primary and secondary alcohols. *Adv Synth Catal* 2004;346:125-

42. DOI
20. Tian K, Li Z. A simple biosystem for the high-yielding cascade conversion of racemic alcohols to enantiopure amines. *Angew Chem Int Ed Engl* 2020;59:21745-51. DOI
21. Albarrán-velo J, Gotor-fernández V, Lavandera I. One-pot two-step chemoenzymatic deracemization of allylic alcohols using laccases and alcohol dehydrogenases. *Mol Catal* 2020;493:111087. DOI
22. González-granda S, Méndez-sánchez D, Lavandera I, Gotor-fernández V. Laccase-mediated oxidations of propargylic alcohols. Application in the deracemization of 1-arylprop-2-yn-1-ols in combination with alcohol dehydrogenases. *ChemCatChem* 2020;12:520-7. DOI
23. Martínez-montero L, Gotor V, Gotor-fernández V, Lavandera I. Stereoselective amination of racemic sec-alcohols through sequential application of laccases and transaminases. *Green Chem* 2017;19:474-80. DOI
24. Méndez-sánchez D, Mangas-sánchez J, Lavandera I, Gotor V, Gotor-fernández V. Chemoenzymatic deracemization of secondary alcohols by using a TEMPO-Iodine-alcohol dehydrogenase system. *ChemCatChem* 2015;7:4016-20. DOI
25. de Gonzalo G, Paul CE. Recent trends in synthetic enzymatic cascades promoted by alcohol dehydrogenases. *Curr Opin Green Sust* 2021;32:100548. DOI
26. Schoemaker HE, Mink D, Wubbolts MG. Dispelling the myths--biocatalysis in industrial synthesis. *Science* 2003;299:1694-7. DOI PubMed
27. Hartmann M, Kostrov X. Immobilization of enzymes on porous silicas--benefits and challenges. *Chem Soc Rev* 2013;42:6277-89. DOI PubMed
28. Gao J, Kong W, Zhou L, et al. Monodisperse core-shell magnetic organosilica nanoflowers with radial wrinkle for lipase immobilization. *Chem Eng J* 2017;309:70-9. DOI
29. Deng J, Wang H, Zhan H, et al. Catalyzed degradation of polycyclic aromatic hydrocarbons by recoverable magnetic chitosan immobilized laccase from *Trametes versicolor*. *Chemosphere* 2022;301:134753. DOI
30. Zheng F, Cui BK, Wu XJ, Meng G, Liu HX, Si J. Immobilization of laccase onto chitosan beads to enhance its capability to degrade synthetic dyes. *Int Biodeter Biodegr* 2016; 10:69-78. DOI
31. Gao J, Wang Y, Du Y, et al. Construction of biocatalytic colloidosome using lipase-containing dendritic mesoporous silica nanospheres for enhanced enzyme catalysis. *Chem Eng J* 2017;317:175-86. DOI
32. Videira-quintela D, Martin O, Montalvo G. Emerging opportunities of silica-based materials within the food industry. *Microchem J* 2021;167:106318. DOI
33. Costantini A, Califano V. Lipase immobilization in mesoporous silica nanoparticles for biofuel production. *Catalysts* 2021;11:629. DOI
34. Kalantari M, Yu M, Yang Y, et al. Tailoring mesoporous-silica nanoparticles for robust immobilization of lipase and biocatalysis. *Nano Res* 2017;10:605-17. DOI
35. Cao G, Gao J, Zhou L, et al. Fabrication of Ni<sup>2+</sup>-nitrilotriacetic acid functionalized magnetic mesoporous silica nanoflowers for one pot purification and immobilization of His-tagged  $\omega$ -transaminase. *BioChem Eng J* 2017;128:116-25. DOI
36. Zhou L, Ouyang Y, Kong W, et al. One pot purification and co-immobilization of His-tagged old yellow enzyme and glucose dehydrogenase for asymmetric hydrogenation. *Enzyme Microb Technol* 2022;156:110001. DOI
37. Li Y, Luan P, Dong L, et al. Asymmetric reduction of conjugated C=C bonds by immobilized fusion of old yellow enzyme and glucose dehydrogenase. *Green Synth Catal* 2022:online ahead of print. DOI
38. Gao L, Wang Z, Liu Y, et al. Co-immobilization of metal and enzyme into hydrophobic nanopores for highly improved chemoenzymatic asymmetric synthesis. *Chem Commun* 2020;56:13547-50. DOI
39. Kong W, Liu Y, Huang C, et al. Direct asymmetric reductive amination of alkyl (hetero)aryl ketones by an engineered amine dehydrogenase. *Angewandte Chemie* 2022;134:e202202264. DOI
40. Demir A, Şeşenoglu Ö, Eren E, et al. Enantioselective synthesis of  $\alpha$ -Hydroxy ketones via benzaldehyde lyase-catalyzed C-C bond formation reaction. *Adv Synth Catal* 2002;344:96-103. DOI
41. Peng B, Ma CL, Zhang P, et al. An effective hybrid strategy for converting rice straw to furoic acid by tandem catalysis via Sn-sepiolite combined with recombinant *E. coli* whole cells harboring horse liver alcohol dehydrogenase. *Green Chem* 2019;21:5914-23. DOI
42. Ghannadi S, Abdizadeh H, Miroliaei M, Saboury AA. Immobilization of alcohol dehydrogenase on titania nanoparticles to enhance enzyme stability and remove substrate inhibition in the reaction of formaldehyde to methanol. *Ind Eng Chem Res* 2019;58:9844-54. DOI
43. Esmailnejad-ahranjani P, Kazemeini M, Singh G, Arpanaei A. Amine-functionalized magnetic nanocomposite particles for efficient immobilization of lipase: effects of functional molecule size on properties of the immobilized lipase. *RSC Adv* 2015;5:33313-27. DOI
44. Zang L, Qiu J, Wu X, Zhang W, Sakai E, Wei Y. Preparation of magnetic chitosan nanoparticles as support for cellulase immobilization. *Ind Eng Chem Res* 2014;53:3448-54. DOI
45. Barbosa O, Ortiz C, Berenguer-murcia Á, Torres R, Rodrigues RC, Fernandez-lafuente R. Glutaraldehyde in bio-catalysts design: a useful crosslinker and a versatile tool in enzyme immobilization. *RSC Adv* 2014;4:1583-600. DOI
46. Songulashvili G, Jimenez-Tobón GA, Jaspers C, Penninckx MJ. Immobilized laccase of *Cerrena unicolor* for elimination of endocrine disruptor micropollutants. *Fungal Biol* 2012;116:883-9. DOI PubMed
47. Zhang J, Xu Z, Chen H, Zong Y. Removal of 2,4-dichlorophenol by chitosan-immobilized laccase from *Coriolus versicolor*. *BioChem Eng J* 2009;45:54-9. DOI



48. Sathishkumar P, Kamala-kannan S, Cho M, et al. Laccase immobilization on cellulose nanofiber: the catalytic efficiency and recycle application for simulated dye effluent treatment. *J Mol Catal B-Enzym* 2014;100:111-20. [DOI](#)
49. Kašpar O, Tokárová V, Nyanhongo GS, Gübitz G, Štěpánek F. Effect of cross-linking method on the activity of spray-dried chitosan microparticles with immobilized laccase. *Food Bioprod Process* 2013;91:525-33. [DOI](#)
50. Li X, Zhu H, Feng J, et al. One-pot polyol synthesis of graphene decorated with size- and density-tunable Fe<sub>3</sub>O<sub>4</sub> nanoparticles for porcine pancreatic lipase immobilization. *Carbon* 2013;60:488-97. [DOI](#)
51. Ida J, Matsuyama T, Yamamoto H. Immobilization of glucoamylase on ceramic membrane surfaces modified with a new method of treatment utilizing SPCP-CVD. *Biochem Eng J* 2000;5:179-84. [DOI](#) [PubMed](#)
52. Grahame DAS, Bryksa BC, Yada RY. Improving and tailoring enzymes for food quality and functionality. Woodhead Publishing; 2015.pp.11-55.
53. Frankenberger W, Johanson J. Effect of pH on enzyme stability in soils. *Soil Biol Biochem* 1982;14:433-7. [DOI](#)
54. Puetz H, Puchlová E, Vranková K, Hollmann F. Biocatalytic oxidation of alcohols. *Catalysts* 2020;10:952. [DOI](#)
55. Lalonde J. Highly engineered biocatalysts for efficient small molecule pharmaceutical synthesis. *Curr Opin Biotechnol* 2016;42:152-8. [DOI](#) [PubMed](#)
56. Paul CE, Lavandera I, Gotor-Fernández V, Kroutil W, Gotor V. *Escherichia coli* /ADH-A: an all-inclusive catalyst for the selective biooxidation and deracemisation of secondary alcohols. *ChemCatChem* 2013;5:3875-81. [DOI](#)
57. Musa MM, Hollmann F, Mutti FG. Synthesis of enantiomerically pure alcohols and amines via biocatalytic deracemisation methods. *Catal Sci Technol* 2019;9:5487-503. [DOI](#) [PubMed](#) [PMC](#)
58. Mutti FG, Knaus T, Scrutton NS, Breuer M, Turner NJ. Conversion of alcohols to enantiopure amines through dual-enzyme hydrogen-borrowing cascades. *Science* 2015;349:1525-9. [DOI](#) [PubMed](#) [PMC](#)
59. Chen FF, Liu YY, Zheng GW, Xu JH. Asymmetric amination of secondary alcohols by using a redox-neutral two-enzyme cascade. *ChemCatChem* 2015;7:3838-41. [DOI](#)